A new method for improved standardisation in three-dimensional computed tomography cephalometry

S. Van Cauter, W. Okkerse, G. Brijs, M. De Beule, M. Braem and B. Verhegghe

In: Computer Methods in Biomechanics and Biomedical Engineering, 13 (1), 59-69, 2010

Link to the article : http://dx.doi.org/10.1080/10255840903014967

Computer Methods in Biomechanics and Biomedical Engineering
Vol. 00, No. 00, May 2008, 1–14

RESEARCH ARTICLE

A new method for improved standardisation in three-dimensional computed tomography cephalometry

S. Van Cauter[a,b*], W. Okkerse[b,c,d], G. Brijs[d], M. De Beule[a,e], M. Braem[b,c] and B. Verhegghe[a,e]

[a]*Institute Biomedical Technology (IBiTech), Ghent University, Ghent, Belgium*; [b]*Lab Dental Materials, Antwerp University, Antwerp, Belgium*; [c]*Department of Dentistry, Antwerp University Hospital, Antwerp, Belgium*; [d]*Department of Oral and Maxillofacial Surgery, Heilige Familie General Hospital, Reet, Belgium*; [e]*Department of Civil Engineering, Ghent University, Ghent, Belgium*

(*Received 00 Month 200x; final version received 00 Month 200x*)

Interest for three-dimensional computed tomography cephalometry has risen over the last two decades. Current methods commonly rely on the examiner to manually point-pick the landmarks and/or orientate the skull. In this study a new approach is presented, in which landmarks are calculated after selection of the landmark region on a triangular model and in which the skull is automatically orientated in a standardised way. Two examiners each performed five analyses on three skull models. Landmark reproducibility was tested by calculating the standard deviation for each observer and the difference between the mean values of both observers. The variation can be limited to 0.1 mm for most landmarks. However, some landmarks perform less and require further investigation. With the proposed reference system a symmetrical orientation of the skulls is obtained. The presented methods contribute to standardisation in cephalometry and could therefore allow improved comparison of patient data.

Keywords: cephalometry; three-dimensional; computed tomography; orthognathic surgery

1. Introduction

Cephalometry is the scientific study of the measurement of the head in relation to specific reference points. Based on these points, which are called anatomical landmarks, various distances, angles, lines and planes are calculated. Since its introduction by Broadbent (Broadbent 1931) and Hofrath (Hofrath et al. 1931) in 1931, cephalometry is a widely used measurement tool for diagnosis, treatment planning and outcome evaluation of dentofacial disharmonies in orthodontics and craniofacial surgery.

Traditionally, the landmarks are identified on tracings of 2D cephalometric radiographs. However, conventional radiographs are characterised by overlap effects due to superimposition of anatomical structures and by magnification and distortion errors depending on the distances between the X-ray source, the object and the film (Bergersen 1980; Friedland 1998; Dibbets and Nolte 2002). Moreover, it has been found that tracing variance is an important source of error (Baumrind and Frantz 1971; Houston et al. 1986; Kamoen et al. 2001). Another disadvantage

*Corresponding author. Email: Sofie.VanCauter@UGent.be

ISSN: 1741-5977 print/ISSN 1741-5985 online

DOI: 10.1080/1741597YYxxxxxxxx
http://www.informaworld.com

is that facial asymmetry in the frontal plane induces significant error in the evaluation of the lateral cephalogram as bilateral structures do not align or superimpose (Hurst et al. 2007). Because of these limitations, three-dimensional (3D) analyses using multiplanar radiography have been proposed (Grayson et al. 1988; Mori et al. 2001), which show better accuracy and reproducibility when compared to 2D cephalometry (Adams et al. 2004). In this case the landmarks should be visible on images obtained from two or more different points of view and the difference in magnification of the various anatomical structures should be corrected.

Three-dimensional computed tomography (3D CT) cephalometry has gained popularity over the last two decades due to the progress in CT imaging and the increased interest for computer-assisted planning of surgery. It has been shown that CT data can provide additional useful information to standard radiography for patient management and that in most of the cases 2D CT scan slices are not as useful without 3D rendered images (Alder et al. 1995; Reuben et al. 2005). Furthermore, distance measurements are more exact using reformatted 3D images than using original 2D slice data (Hildebolt et al. 1990; Frühwald et al. 2008). With the aid of 3D computed tomography, the model can be viewed from any angle, the inner structures can be visualised and various organs can be observed independently (Park et al. 2006). In addition, 3D CT cephalometry allows evaluation of complex abnormal anatomies such as asymmetrical cases since three-dimensional images and measurements are assessed (Hwang et al. 2006; Rooppahkun et al. 2006). Finally, compared to 2D radiographic cephalometry, intra- and inter-observer reproducibilities are significantly superior following the 3D CT method (Olszewski et al. 2007).

The anatomical landmarks or cephalometric points are commonly determined by manual point-picking on these surface renderings. Because of the variability in the head position during scanning, orientation of the image is required. This is done either by manual (subjective) alignment of anatomical structures or by automatic set-up of a reference system based on previously determined landmarks. Consequently, reproducibility depends mainly on the judgement and experience of the examiner.

Cephalometric analysis can be used to evaluate the outcome of orthognathic surgery, in which the position of one or more jawbones is corrected. Reproducibility of the landmark coordinates should be high to allow for correct comparison of data such as pre- and postoperative images. Otherwise, the variability in measurement values could lead to misinterpretation of the data, especially when the jaws were moved rather little during surgery. In this paper, new methods for landmark identification and image orientation are investigated, which aim to improve reproducibility of cephalometric measurements. The approach which is used is twofold: advance standardisation in cephalometry and limit the input of the examiner.

2. Materials and methods

The new methods for improved standardisation in 3D CT cephalometry were developed using pyFormex (http://pyformex.berlios.de), which is an open-source program under development at IBiTech. This software is intended for generating, manipulating and operating on large geometrical models of 3D structures. A module for cephalometric analysis was created combining general features of pyFormex and newly implemented tools for landmark identification and image orientation. All operations are performed on a triangular model of the skull.

Table 1. Landmarks used in this study. Biological landmarks (type B) are defined by a surface and/or line region and direction. Constructed landmarks (type C) are defined by their construction method.

Landmark	Type	Surface region	Line region	Direction/ Construction
OrR	B	Lower part of right orbit	Highest points of sagittal profiles	Inferior
OrL	B	Lower part of left orbit	Highest points of sagittal profiles	Inferior
N	B	Part of nasal and frontal bone	Deepest points of sagittal profiles	Anterior
CAR	B	Right posterior angle of lesser wing		Posterior
CAL	B	Left posterior angle of lesser wing		Posterior
CPR	B	Right anterior angle of dorsum sellae		Anterior
CPL	B	Left anterior angle of dorsum sellae		Anterior
SS	C			Mean of Clinoid points
SI	B	Hypophyseal fossa	Sagittal profile through SS	Inferior
S	C			Mean of SS and SI

2.1 Landmark identification

The cephalometric points determined in this study are summarised in Table 1. Two types of points can be distinguished: biological (type B) and constructed (type C) landmarks. Biological landmarks are situated on a certain anatomical structure of the body. In this work, they are identified by calculating the extreme point in a specified direction of the structure. This is illustrated in Figure 1 for the point Orbitale Right (OrR), which is defined in the literature as the most inferior point of the right infra-orbital rim. The following procedure is carried out to determine OrR:

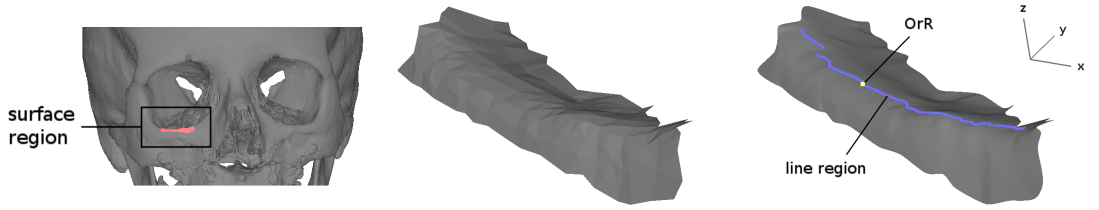

(a) The user picks a surface region on the triangular model.

(b) The original surface region is quite coarse.

(c) The surface region is smoothed and refined, a line region is calculated and the landmark is determined.

Figure 1. Landmark determination illustrated for the point OrR.

- *The examiner selects a surface region on the triangular model of the skull.*
  For this operation, a picking procedure was developed which allows the user to (de)select triangles, remove unconnected parts from the selection and refine the selection in a new picking operation. For the landmark OrR, the surface region is the lower part of the right orbit (see Figure 1a).
- *The quality of the surface region is improved.*
  As shown in Figure 1b, the triangular surface model is quite coarse. Therefore, some quality improving techniques are performed.
  - The surface region is smoothed to remove noise and to obtain a more uniform curvature.
  The vertices (corner points of the triangles) are submitted to a low-pass filter algorithm (Taubin 1995, 2000), which is a combination of two Laplace filters. During Laplacian smoothing, the vertex coordinates are recalculated according to Equation 1, in which p are the original coordinates, n is the valence (number of edges connected to p), q_i are the adjacent points (points that share an edge with p) and λ is a scale factor ($0 < \lambda < 1$). However, the object tends to shrink drastically after applying the Laplace filter iteratively a large number of times.

In Figure 2a, the Laplace filter for a scale factor λ of 0.5 and four iterations is shown. In this figure, k are the frequencies of the surface signal ($0 \leq k \leq 2$) and f(k) is the transfer function of the filter. Low frequencies correspond to low curvatures, while high frequencies correspond to high curvatures. The Laplace filter produces shrinkage because all the frequency components, other than the zero component are attenuated ($|f(k)| < 1$ for $0 < k \leq 2$).

To prevent shrinkage, the low-pass filter alternates between two steps of Laplacian smoothing: a shrinking step with the positive scale factor λ and an unshrinking step with the negative scale factor μ, greater than λ in absolute value ($\mu < -\lambda < 0$). As shown in Figure 2b, this filter preserves low frequency components ($0 \leq k \leq k_{PB}$) and attenuates higher frequency components ($k_{PB} < k \leq 2$). The boundary is the pass-band frequency k_{PB} ($f(k_{PB}) = 1$). If the scale factor λ and the pass-band frequency k_{PB} are known, μ can be calculated from Equation 2. As suggested by Taubin, a pass-band frequency of 0.1 was chosen. The surface region is smoothed using four iterations of a low-pass filter with a scale factor λ of 0.5. For this combination of parameters, the transfer function f(k) decreases to zero, as k increases from $k = k_{PB}$ to $k = 2$ (see Figure 2b).

The surface regions of one skull model before and after low-pass filtering were compared to evaluate the error induced by smoothing. Since the regions are not closed, the volume change could not be used as an appropriate measure for shrinkage and the change in the surface area was used instead. The area change varied between -0.23% and -1.16% and is therefore negligible. As a comparison, the analogous Laplace filter would result in an area change between -0.82% and -13.46%.

$$p' = p + \frac{\lambda}{n} \sum_{i=0}^{n-1} (q_i - p) \tag{1}$$

$$\frac{1}{\lambda} + \frac{1}{\mu} = k_{PB} \tag{2}$$

- The surface region is refined to allow for interpolation between the original vertices of the model.

For this step, a subdivision algorithm based on the modified butterfly scheme (Zorin et al. 1996; Zorin and Schröder 2000) was implemented. This algorithm splits every triangle into four new triangles by inserting one vertex per edge. The new vertex is calculated as a weighted sum of vertices adjacent to the edge. The weights depend on the characteristics of the edge (boundary or interior edge, boundary or interior vertices, valence of the vertices) and, in total, eight rules can be distinguished. The modified butterfly scheme guaranties that the limit surface is C1 continuous, i.e. has continuous tangent planes (Zorin 1997). The surface region is refined using three iterations of the subdivision algorithm.

The model resulting from the smoothing and refinement operation is shown in Figure 1c.

- *A line region is calculated.*

In this case, the line region approximates the infra-orbital rim. It is defined as the highest points of sagittal (yz) profiles through the surface region (see Figure 1c). The distance between these profiles is approximately 0.05 mm. Since not all

landmark definitions include a line region, this step is optional.

- *The landmark coordinates are determined.*
  For the point OrR, the lowest point of the line region is calculated (see Figure 1c). For landmarks which do not have a line region, the extreme point of the surface region is calculated.

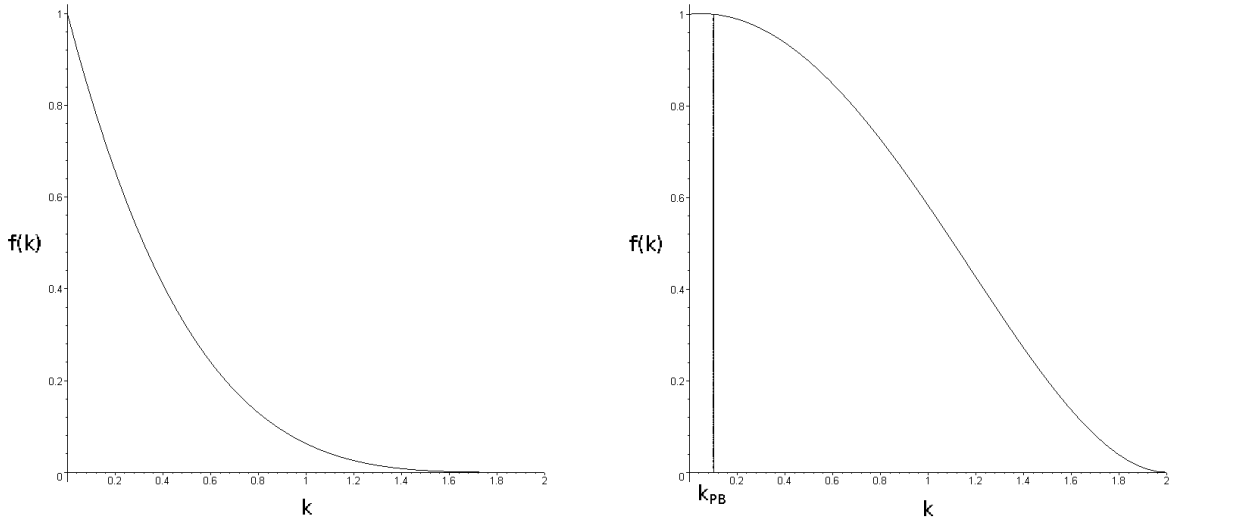

(a) Laplace filter: $f(k) = (1 - \lambda k)^n$ ($\lambda = 0.5$, $n = 4$)

(b) Low-pass filter: $f(k) = ((1 - \lambda k)(1 - \mu k))^{n/2}$ ($\lambda = 0.5$, $n = 4$, $k_{PB} = 0.1$)

Figure 2. Different smoothing filters: k are the frequencies of the surface signal ($0 \leq k \leq 2$) and f(k) is the transfer function of the filter. Low frequencies correspond to low curvatures, while high frequencies correspond to high curvatures.

This approach restricts the input of the user to the selection of the surface region on the triangular model of the skull. All the following steps are performed automatically. Other biological landmarks used in this study are points Orbitale Left (OrL), Nasion (N), Clinoid (CAR, CAL, CPR, CPL) and Sella Inferior (SI). As shown in Table 1, these points are defined by the anatomical structure (surface and/or line region) on which they are situated and by the direction in which they are calculated as the extreme point. The position of the landmarks is depicted in Figure 3.

Constructed landmarks are defined using a combination of other landmarks. As an example, the construction of the point Sella (S) is explained. This landmark is traditionally defined as the centre of the sella turcica, which is a saddle-shaped depression in the sphenoid bone (see Figure 3b and c). It is computed by the following procedure:

- Four Clinoid points are determined: two on the lesser wing and two on the dorsum sellae (see Table 1 and Figure 3b).
- Landmark Sella Superior (SS) is calculated as the mean of the four Clinoid points (see Figure 3c).
- Landmark SI is determined as the lowest point of the intersection of the hypophyseal fossa (seat of the sella turcica) with a sagittal plane through SS (see Figure 3b and c).
- Landmark S is calculated as the mean of SS and SI (see Figure 3c).

Both constructed points used in this study, SS and S, are again calculated automatically.

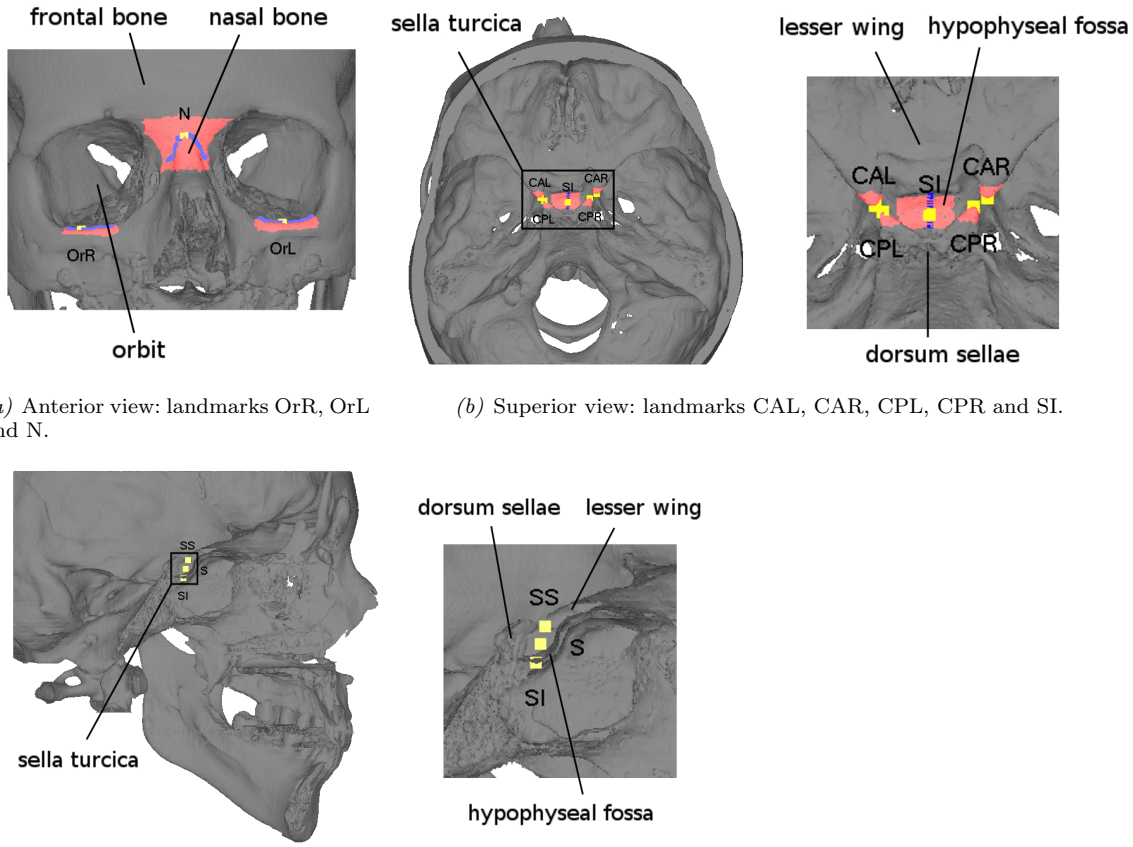

(a) Anterior view: landmarks OrR, OrL and N.

(b) Superior view: landmarks CAL, CAR, CPL, CPR and SI.

(c) Paramedian sagittal view: landmarks SS, SI and S.

Figure 3. Landmarks used in this study. The surface regions (red), line regions (blue) and points (yellow) are visualised.

2.2 Image orientation

To orientate the model, a reference system based on four landmarks is set up: OrR, OrL, S and N. During image orientation, four requisites are taken into account, which correspond to three rotations and one translation (see Table 2). The rotation in the frontal and transversal planes aims to obtain an orientation in which similar anatomical structures are positioned symmetrically relative to the mid-sagittal (yz) plane. This is the natural head position, which, in addition, will result in landmarks which are most clinically meaningful. For example, point N will be situated more in the middle of the nasal bone along the transversal (x) axis if the skull is positioned symmetrically. To obtain such an orientation, OrR and OrL are placed at the same height and S and N are positioned in the same sagittal plane. Rotation in the sagittal plane puts the anterior cranial base (S-N line) six degrees above the horizontal plane. This transformation is based on the two- to nine-degree average orientation of the S-N line from true horizontal (Madsen et al. 2008). Finally, point S is positioned at the origin. The reference system is visualised in Figure 4. Since all transformations are based on previously determined landmarks, the orientation procedure can be performed automatically.

Because after rotating the skull the extreme points may have changed, the line regions and landmark coordinates have to be recalculated. Since this may result in a different reference system, image orientation has to be repeated as well. Hence, an iterative procedure is used. During each iteration, the skull is re-orientated and the line regions and landmarks are recalculated. After each iteration, the four

Table 2. Orientation requisites used to set up the reference system.

Transformation	Requisite
Rotation in the frontal plane	OrR and OrL at the same height
Rotation in the transversal plane	S-N line in a sagittal plane
Rotation in the sagittal plane	S-N line six degrees above the horizontal plane
Translation	S at the origin

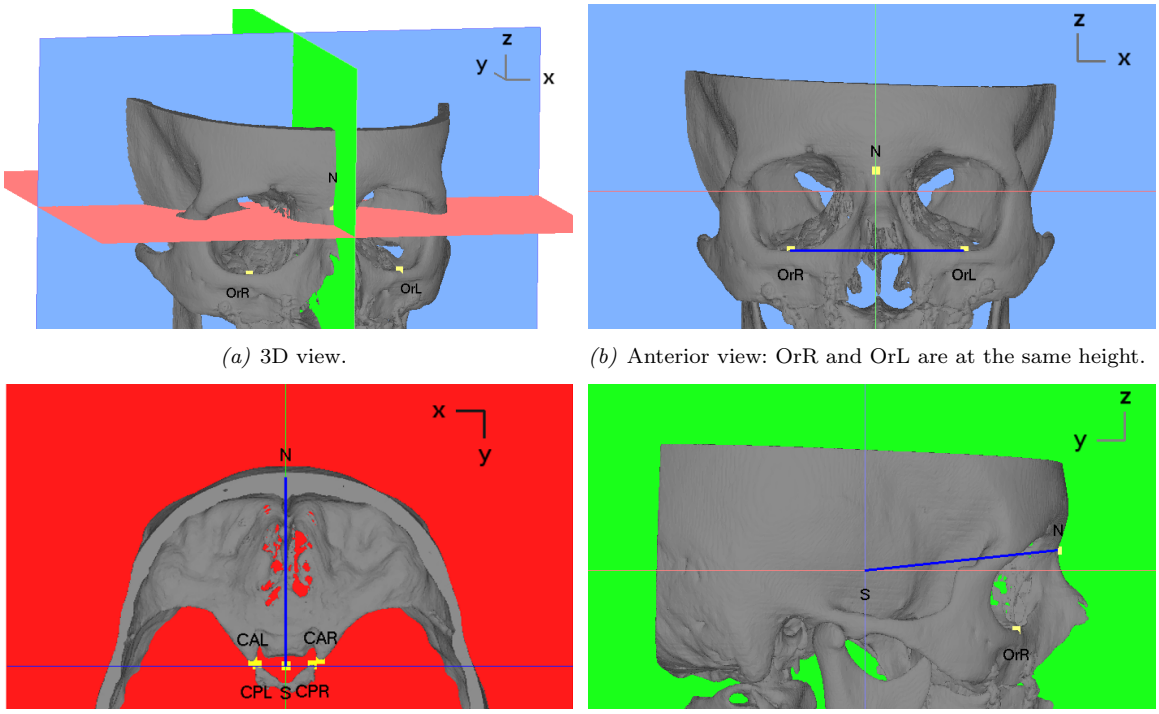

(a) 3D view.

(b) Anterior view: OrR and OrL are at the same height.

(c) Superior view: the S-N line is positioned in the mid-sagittal plane.

(d) Lateral view: the S-N line is situated six degrees above the horizontal plane.

Figure 4. The reference system used to orientate the skull (x, transversal axis; y, sagittal axis; z, longitudinal axis).

orientation requisites of Table 2 are evaluated. The orientation procedure stops when all requisites are fulfilled. In this case, the three rotation angles associated with these requisites have converged to zero. However, due to the character of the model, only a finite number of vertices can be taken into account. As a result, it is possible that the orientation procedure does not converge, i.e. that one or more rotation angles do not converge to zero. Instead, consecutive angles which have the same absolute value but different sign can be observed. Therefore, the procedure stops after equal rotation angles are detected in three iterations. To decrease the deviation from a converged referenced system, a last iteration is performed, in which the skull is rotated over angles that are half of the recurrent rotation angles in absolute value. In this case, a warning message is shown to the user and the final deviation (the deviation of the current reference system from the reference system set up by the final landmark coordinates) can be viewed.

2.3 Evaluation of the new methods

To study the performance of the new methods, three sets of CT scans were used. All images had an intra-slice resolution of 0.48 mm and inter-slice resolution of 0.6 mm. Segmentation and 3D reconstruction of the skull was done using Mimics® (Materialise NV, Leuven, Belgium). The predefined threshold interval for bone in

CT images (226–3071 HU) was chosen to identify the skull and the optimal quality parameters were selected to calculate a triangular surface mesh. Then, the 3D surface model was loaded into pyFormex.

Using the cephalometry module, two examiners each performed five analyses for the three skull models, with a minimum time interval of two days. Based on these data, the orientation of the skull models and the reproducibility of the landmark coordinates were investigated. To evaluate the orientation method, a quantitative judgement of the symmetrical appearance of the models was made. Since all data were obtained from patients undergoing orthognathic surgery, the jaws are likely to have an asymmetrical position and thus they were removed from the skull model. Next, the model was split into two parts, separated by the mid-sagittal (yz) plane. The positive vertices were mirrored against the mid-sagittal plane and the minimum distance of each mirrored positive vertex from the negative vertices was calculated. Finally, the percentage of mirrored positive vertices lying within a certain distance from the negative vertices was determined. Intra-observer reproducibility was examined by means of the standard deviation of the five analyses of each user. Inter-observer reproducibility was evaluated by calculating the difference between the mean values of the five analyses of each observer.

3. Results

3.1 Orientation

The orientation of the skull models after calculation of the reference system is shown in Figure 5. A symmetrical orientation relative to the mid-sagittal (yz) plane can be observed for the three models. The percentage of mirrored positive vertices lying within a certain distance from the negative vertices is shown in Figure 6. Fifty per cent of the mirrored positive vertices lies within 0.8 mm, 75% within 1.3 mm and 90% within 2.2 mm from the negative vertices. The mean calculation time for the orientation procedure was approximately 6 min. Two calculations did not converge, but this did not result in a significant error since the maximum deviation of the final reference system from the reference system set up by the final landmark coordinates was -0.03 degrees.

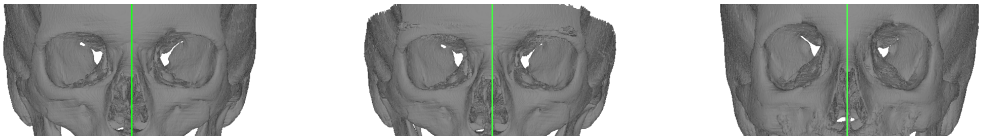

(a) Model 1. *(b)* Model 2. *(c)* Model 3.

Figure 5. The skull models after the calculation of the reference system. A symmetrical orientation relative to the mid-sagittal (yz) plane is obtained.

3.2 Intra-observer reproducibility

Intra-observer reproducibility is depicted in Figures 7 and 8. The standard deviations of the 10 landmarks along the transversal (x), sagittal (y) and longitudinal (z) axis before and after the orientation procedure were calculated.

For the first examiner, all landmarks except OrL and OrR have standard deviations below 0.1 mm, which indicates high reproducibility. The higher values for

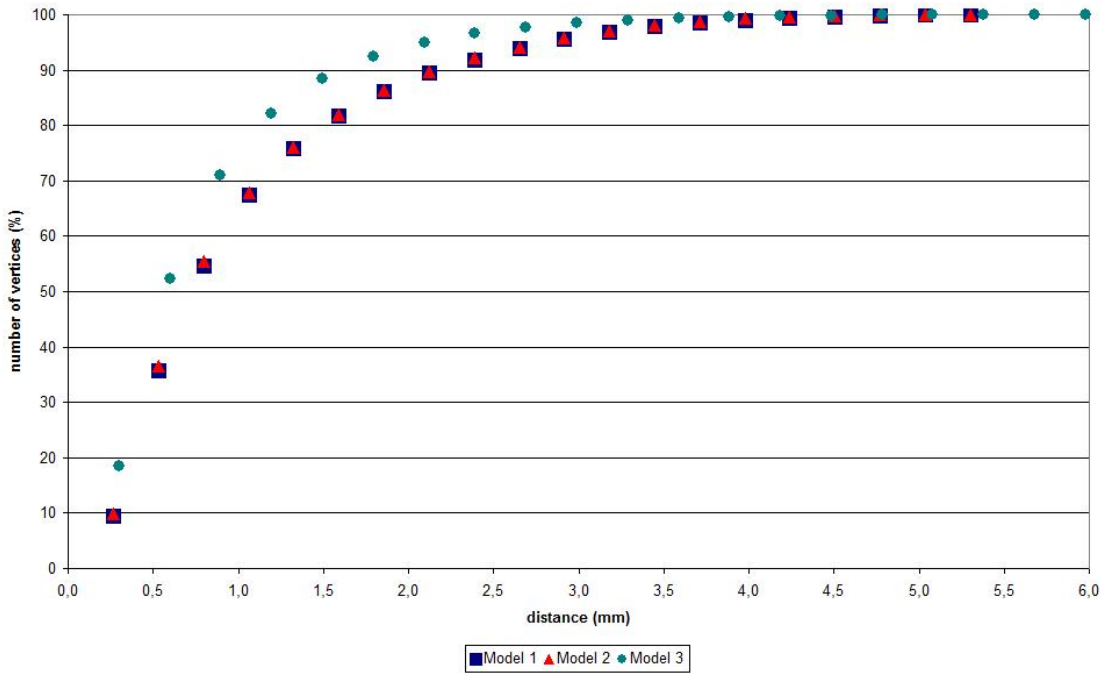

Figure 6. Quantitative evaluation of the symmetrical appearance of the models: the percentage of mirrored positive vertices lying within a certain distance from the negative vertices.

the Orbitale points can be explained as follows. In the second model, the line region for OrL is rather horizontal in the neighbourhood of the lowest point before orientation. As a result, a higher standard deviation (0.96 mm) was obtained for the x-coordinate of the landmark. After orientation however, all values are below 0.22 mm. The results for the third model show high variability for the points OrL and OrR, before as well as after the calculation of the reference system. This is caused by the fact that the infra-orbital rim can not be readily distinguished. If the surface region not clearly goes up and down in the sagittal (y) direction (see Figure 1c), then the result for the line region, which was defined as the highest points of sagittal (yz) profiles through the surface region, will depend on the area to which the surface region extends in the sagittal direction. Consequently, high standard deviations occur in the sagittal direction for the points OrL and OrR (0.85 mm and 1.82 mm after orientation).

Similar results are obtained for the second examiner. In the first and second model, 8 out of 10 landmarks have standard deviations below 0.1 mm, while the points OrL and OrR have standard deviations below 0.46 mm and 0.29 mm. The highest variability is again observed for the third model, in particular for points OrL and OrR (3.40 mm and 1.70 mm after orientation).

3.3 Inter-observer reproducibility

Inter-observer reproducibility is shown in Figure 9. The difference between the mean values of both examiners is below 0.1 mm for all landmarks except OrL and OrR in the three models. The highest values for OrL and OrR are 0.43 mm and 0.05 mm in the first model, 0.49 mm and 0.34 mm in the second model and 1.46 mm and 2.81 mm in the third model.

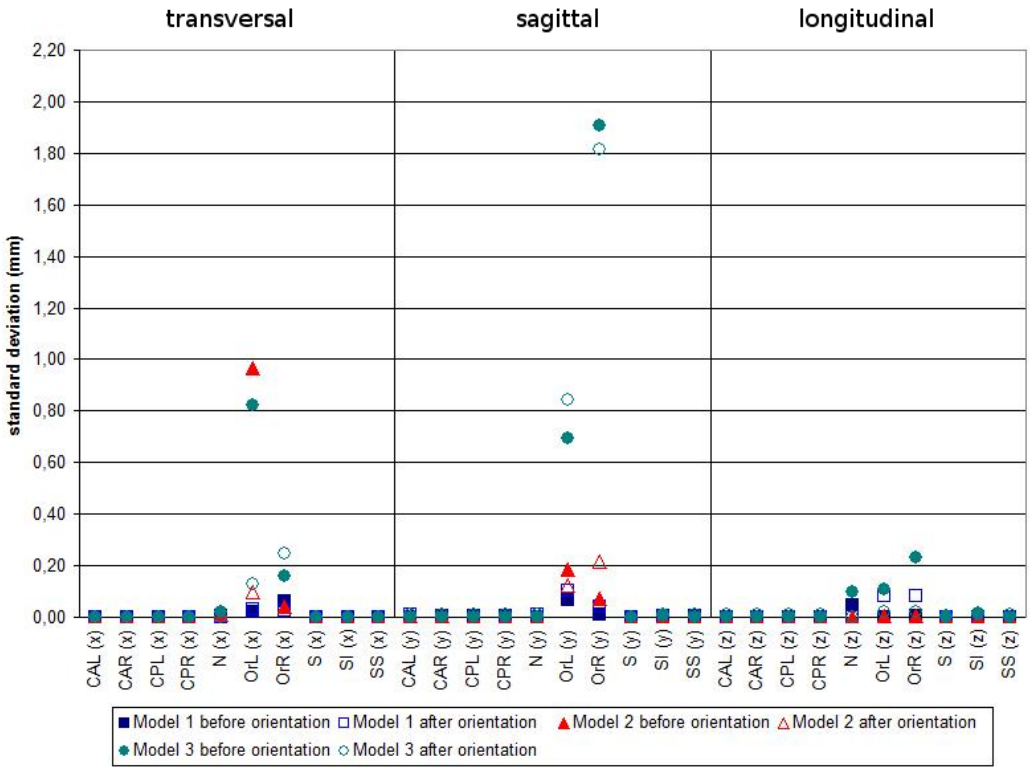

Figure 7. Intra-observer reproducibility for examiner 1: standard deviation of five analyses along the transversal (x), sagittal (y) and longitudinal (z) axis.

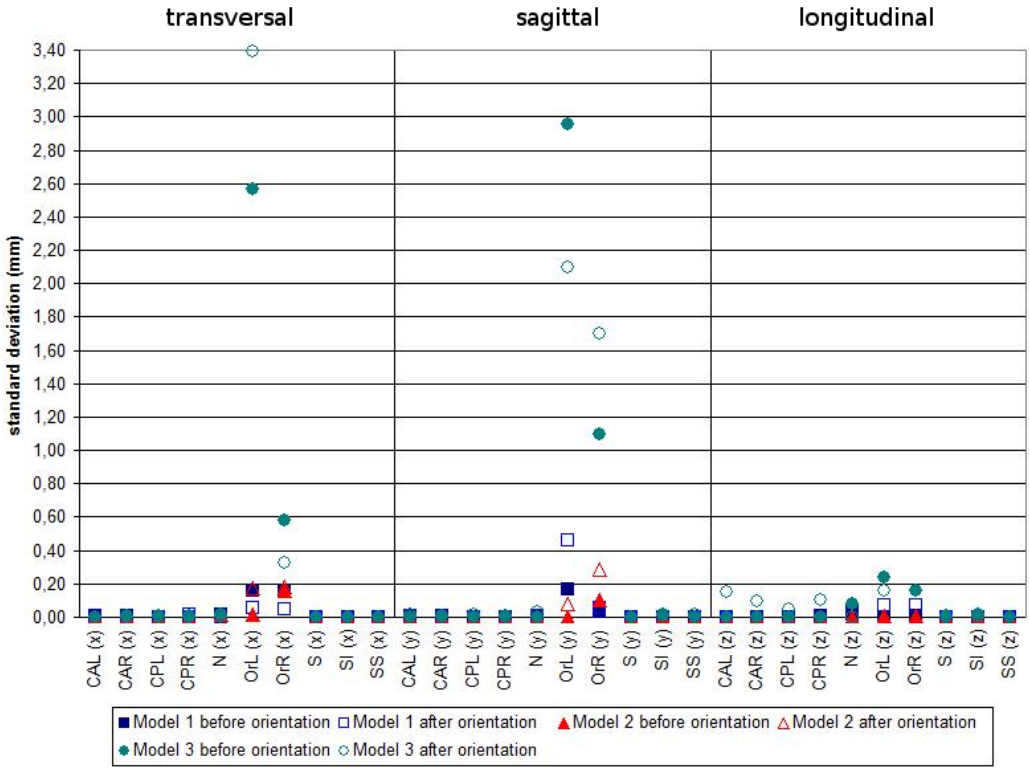

Figure 8. Intra-observer reproducibility for examiner 2: standard deviation of five analyses along the transversal (x), sagittal (y) and longitudinal (z) axis.

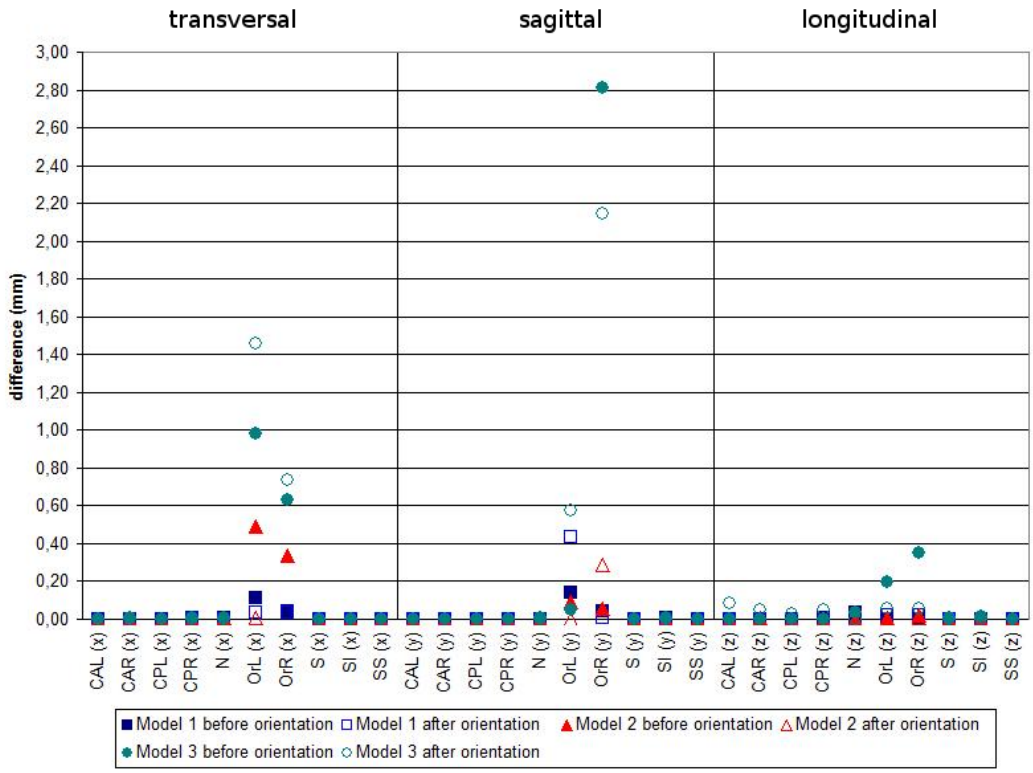

Figure 9. Inter-observer reproducibility: difference between the mean values of both examiners along the transversal (x), sagittal (y) and longitudinal (z) axis.

4. Discussion

Many studies regarding 3D CT cephalometry have been performed, presenting various methods for landmark identification, image orientation (Haffner et al. 1999; Lagravère et al. 2006; Park et al. 2006; Swennen et al. 2006) and cephalometric analysis (Bettega et al. 2000; Olszewski et al. 2006; Park et al. 2006) and showing the need for improved standardisation and for the investigation of the accuracy and reproducibility of cephalometric measurements. Several studies about reproducibility of 3D CT cephalometry have been published. Some of them investigated correlation coefficients, while others calculated standard deviations. Intra-observer intraclass correlation coefficients between 0.970 and 0.998 for 10 subjects and four landmarks (Lagravère et al. 2006) and between 0.941 and 0.993 for 23 subjects and 20 linear distances (Periago et al. 2008) have been reported. Intra- and inter-observer intraclass correlation coefficients for 26 subjects and nine linear distances were obtained with 3D CT cephalometry and 2D radiographic cephalometry (Olszewski et al. 2007). The 3D method proved to be significantly superior, showing intra-observer correlation coefficients between 0.9717 and 0.9984 and inter-observer correlation coefficients between 0.9362 and 0.9965. Maximal intra-observer standard deviations of 0.86, 0.93 and 1.67 mm for the transversal, sagittal and longitudinal direction for one subject and 19 landmarks (Park et al. 2006) have been reported. Mean intra-observer standard deviations were 0.39, 0.45 and 0.74 mm.

These studies rely on the examiner to manually point-pick the landmarks and/or orientate the skull. The method for landmark determination presented in this paper limits the input of the user to the selection of a surface region on the skull model. Since this operation is less user-dependent, higher reproducibility can be achieved. In this study, intra-observer standard deviations and inter-observer dif-

ferences lower than 0.1 mm were obtained for most landmarks. When compared to the intra-observer standard deviations reported by Park et al., these results indicate that a significant improvement can be achieved with the new methods. Nevertheless, some landmarks perform poor if the feature that distinguishes them is not present in the geometry. This is, for example, the case for the Orbitale points, if the infra-orbital rim can not be approximated using the definition of the line region. When using the manual point-picking method, however, the user has to deal with the absence of characteristic features on the surface rendering as well. Such landmarks require further investigation. An automated procedure is used to orientate the skull based on four landmarks. Taking into account the method used for landmark determination, an iterative procedure is required to compensate for variations due to rotating the skull. The results obtained in this study show that a symmetrical orientation is achieved with the presented reference system. The distance between the mirrored left part and the right part of the skull is less than 2.2 mm for 90% of the vertices. When evaluating the orientation of the skull models, it should be kept in mind that some skulls may have asymmetrical features, that no skull is completely symmetrical and that the reproducibility of the orientation should be the most determining factor for choosing the reference system.

Cephalometric measurements can be used to evaluate the outcome of a treatment if a correct interpretation of the data is possible. If the observed values of a clinical study are, however, smaller than the reported error, it cannot be concluded that the observed effect is due to therapy (Kamoen et al. 2001). This study shows that the error in landmark determination on 3D surface models can be limited. Moreover, the set-up of a standardised reference system should contribute to the comparison of data, such as pre- and postoperative images from orthognathic patients.

Although interesting preliminary results were obtained in this study, some limitations remain. The number of patient data and landmarks used in this work was rather small. Reproducibility should be tested for a larger amount of data and other landmarks should be investigated. Because of the lower reproducibility of the Orbitale points, other reference systems should be evaluated as well. The accuracy of the landmark coordinates was not studied. In future, landmark coordinates measured on 3D CT models and dry skulls or on 3D models created from different CT images will be compared to study the accuracy of the new methods. The number of smoothing and subdivision steps applied on the surface regions was chosen arbitrarily. The influence of smoothing and subdivision on the accuracy of the landmark coordinates could be used to determine an optimal number of iterations. The main drawback of CT imaging is the increased radiation exposure compared to conventional radiography, but it is shown that with cone beam CT, the radiation dose can be significantly reduced (Loubele et al. 2008). Therefore, cone beam CT will probably enhance the use of 3D CT cephalometry in orthodontic and craniofacial applications.

5. Conclusions

The number of studies concerning 3D CT cephalometry shows that this technique will become an important measurement tool in orthodontics and craniofacial surgery. The methods proposed in this study, namely landmark calculation and image orientation, contribute to an improved standardisation in cephalometry. Because the region-picking operation is less user-dependent, high reproducibility can be achieved for most of the investigated landmarks. Along with the set-up of a standardised reference system, this approach could allow improved comparison of patient data.

Acknowledgement

This research has been funded by the university of Antwerp.

References

Adams GL, Gansky SA, Miller AJ, Harrell WE Jr, Hatcher DC. 2004. Comparison between traditional 2-dimensional cephalometry and a 3-dimensional approach on human dry skulls. Am J Orthod Dentofacial Orthop. 126(4):397–409.

Alder ME, Deahl ST, Matteson SR. 1995. Clinical usefulness of two-dimensional reformatted and three-dimensionally rendered computerized tomographic images: literature review and a survey of surgeons' opinions. J Oral Maxillofac Surg. 53(4):375–386.

Baumrind S, Frantz RC. 1971. The reliability of head film measurements. 1. Landmark identification. Am J Orthod. 60(2):111–127.

Bergersen EO. 1980. Enlargement and distortion in cephalometric radiography: compensation tables for linear measurements. Angle Orthod. 50(3):230–244.

Bettega G, Payan Y, Mollard B, Boyer A, Raphaël B, Lavallée S. 2000. A simulator for maxillofacial surgery integrating 3D cephalometry and orthodontia. Comput Aided Surg. 5(3):156–165.

Broadbent BH. 1931. A new X-ray technique and its application to orthodontia. Angle Orthod. 1(2):45–66.

Dibbets JM, Nolte K. 2002. Effect of magnification on lateral cephalometric studies. Am J Orthod Dentofacial Orthop. 122(2):196–201.

Friedland B. 1998. Clinical radiological issues in orthodontic practice. Semin Orthod. 4(2):64–78.

Frühwald J, Schicho KA, Figl M, Benesch T, Watzinger F, Kainberger F. 2008. Accuracy of craniofacial measurements: computed tomography and three-dimensional computed tomography compared with stereolithographic models. J Craniofac Surg. 19(1):22–26.

Grayson B, Cutting C, Bookstein FL, Kim H, McCarthy JG. 1988. The three-dimensional cephalogram: theory, technique, and clinical application. Am J Orthod Dentofacial Orthop. 94(4):327–337.

Haffner CL, Pessa JE, Zadoo VP, Garza JR. 1999. A technique for three-dimensional cephalometric analysis as an aid in evaluating changes in the craniofacial skeleton. Angle Orthod. 69(4):345–348.

Hildebolt CF, Vannier MW, Knapp RH. 1990. Validation study of skull three-dimensional computerized tomography measurements. Am J Phys Anthropol. 82(3):283–294.

Hofrath H . 1931. Die bedeutung der rntgenfern- und abstandsaufnahme fr die diagnostik der kieferanomalien. J Orofac Orthop. 1(2):232–258.

Houston WJ, Maher RE, McElroy D, Sherriff M. 1986. Sources of error in measurements from cephalometric radiographs. Eur J Orthod. 8(3):149–151.

Hurst CA, Eppley BL, Havlik RJ, Sadove AM. 2007. Surgical cephalometrics: applications and developments. Plast Reconstr Surg. 120(6):92e–104e.

Hwang HS, Hwang CH, Lee KH, Kang BC. 2006. Maxillofacial 3-dimensional image analysis for the diagnosis of facial asymmetry. Am J Orthod Dentofacial Orthop. 130(6):779–785.

Kamoen A, Dermaut L, Verbeeck R. 2001. The clinical significance of error measurement in the interpretation of treatment results. Eur J Orthod. 23(5):569–578.

Lagravère MO, Hansen L, Harzer W, Major PW. 2006. Plane orientation for standardization in 3-dimensional cephalometric analysis with computerized tomography imaging. Am J Orthod Dentofacial Orthop. 129(5):601–604.

Loubele M, Bogaerts R, Van Dijck E, Pauwels R, Vanheusden S, Suetens P, Marchal G, Sanderink G, Jacobs R. 2008. Comparison between effective radiation dose of CBCT and MSCT scanners for dentomaxillofacial applications. Eur J Radiol. doi:10.1016/j.ejrad.2008.06.002.

Madsen DP, Sampson WJ, Townsend GC. 2008. Craniofacial reference plane variation and natural head position. Eur J Orthod. 30(5):532–540. Epub 2008 Jul 16.

Mori Y, Miyajima T, Minami K, Sakuda M. 2001. An accurate three-dimensional cephalometric system: a solution for the correction of cephalic malpositioning. J Orthod. 28(2):143–149.

Olszewski R, Cosnard G, Macq B, Mahy P, Reychler H. 2006. 3D CT-based cephalometric analysis: 3D cephalometric theoretical concept and software. Neuroradiology. 48(11):853–862. Epub 2006 Sep 29.

Olszewski R, Zech F, Cosnard G, Nicolas V, Macq B, Reychler H. 2007. Three-dimensional computed tomography cephalometric craniofacial analysis: experimental validation in vitro. Int J Oral Maxillofac Surg. 36(9):828–833. Epub 2007 Sep 6.

Park SH, Yu HS, Kim KD, Lee KJ, Baik HS. 2006. A proposal for a new analysis of craniofacial morphology by 3-dimensional computed tomography. Am J Orthod Dentofacial Orthop. 129(5):600.e23–600.e34.

Periago DR, Scarfe WC, Moshiri M, Scheetz JP, Silveira AM, Farman AG. 2008. Linear accuracy and reliability of cone beam CT derived 3-dimensional images constructed using an orthodontic volumetric rendering program. Angle Orthod. 78(3):387–395.

Reuben AD, Watt-Smith SR, Dobson D, Golding SJ. 2005. A comparative study of evaluation of radiographs, CT and 3D reformatted CT in facial trauma: what is the role of 3D? Br J Radiol. 78(927):198–201.

Rooppakhun S, Piyasin S, Sitthiseriprati K, Ruangsitt C, Khongkankong W. 2006. 3D CT Cephalometric: A Method to Study Cranio-Maxillofacial Deformities. Papers of Technical Meeting on Medical and Biological Engineering. 6(75-94):85–89.

Swennen GR, Schutyser F, Barth EL, De Groeve P, De Mey A. 2006. A new method of 3-D cephalometry Part I: the anatomic Cartesian 3-D reference system. J Craniofac Surg. 17(2):314–325.

Taubin G. 1995. A signal processing approach to fair surface design. Paper presented at: SIGGRAPH '95. Proceedings of the 22nd Annual Conference on Computer Graphics. Los Angeles, CA, USA, 6-11 August, p. 351–358.

Taubin G. 2000. Geometric signal processing on polygonal meshes. Eurographics 2000. State of the art report. Interlaken, Switzerland, 21-25 August.

Zorin D, Schröder P, Sweldens W. 1996. Interpolating subdivision for meshes with arbitrary topology. Paper presented at: SIGGRAPH '96. Proceedings of the 23rd Annual Conference on Computer Graphics. New Orleans, LA, USA, 4-9 August, p. 189–192.

Zorin D. 1997. [Pasadena, California, USA]: California Institute of Technology. Subdivision and Multiresolution Surface Representations [PhD thesis].

Zorin D, Schröder P. 2000. Subdivision for modeling and animation. SIGGRAPH 2000. Course notes of the 27th Annual Conference on Computer Graphics. New Orleans, LO, USA, 23-28 July.